

# The relevance of the three dimensional Thirring coupling at finite temperature and density\*

R. Narayanan

*Department of Physics, Florida International University, Miami, FL 33199.*

(Dated: June 2, 2020)

## Abstract

We studied the three dimensional Thirring model in the limit of infinite number of flavors at finite temperature and density. We calculated the number density as a function of temperature and the density at zero temperature serves as a relevant parameter. A three dimensional free fermion gas behavior as the density at zero temperature approaches zero smoothly crosses over to a two dimensional free fermion gas behavior as the density at zero temperature approaches infinity.

arXiv:2006.00608v1 [hep-th] 31 May 2020

---

\* *A joyous exercise using polylogarithms and related special functions performed in isolation.*

## I. INTRODUCTION AND SUMMARY

The three dimensional Euclidean (two spatial and one thermal) Thirring model with  $N$  flavors of two-component fermions would have been deemed non-renormalizable by a standard power counting argument but it has been shown to be renormalizable in a  $\frac{1}{N}$  expansion [1–5]. Recently, this strongly coupled theory has been extensively studied to explore the possibility of mass generation [6–20]. With the possible exception of the  $N = 1$  model, a spontaneous generation of mass is most likely ruled out. A numerical analysis of QED in three dimensions has also resulted in similar observations [21–25] but monopoles present in QED can become relevant [26].

In this paper, we explore the relevance of the Thirring coupling in the large  $N$  limit at finite temperature and density. We consider only the massless theory owing to the previous analysis of spontaneous mass generation. The physics at zero temperature has been briefly sketched out in [27]. The effective action in the large  $N$  limit after introducing the standard vector auxiliary field is complex for a non-zero chemical potential and this leads us to perform a saddle point analysis. There are several saddle points at a fixed chemical potential and temperature but we will provide a graphical proof that only one particular saddle point dominates all all values of chemical potential and temperature.

Let  $T$  and  $\mu$  stand for the temperature and chemical potential measured in units of inverse of the Thirring coupling per flavor,  $\lambda$ . We will show that the number density at zero temperature in units of  $\lambda$  is

$$\mathbf{n}_0 = \mu + 2\pi \left( 1 - \sqrt{1 + \frac{\mu}{\pi}} \right), \quad (1)$$

and can be used to set the chemical potential. The relevance of the Thirring coupling is already seen by noticing that the number density at zero temperature smoothly crosses over from  $\frac{\mu^2}{4\pi}$  as  $\mu \rightarrow 0$  to  $\mu$  as  $\mu \rightarrow \infty$ . Defining a reduced temperature by  $T = \sqrt{4\pi\mathbf{n}_0}t$  and writing the number density as a function of temperature as  $\bar{\mathbf{n}}(\mathbf{n}_0, t)\mathbf{n}_0$ , we will show that  $\bar{\mathbf{n}}(\mathbf{n}_0, t)$  is the solution to

$$\bar{\mathbf{n}}(\mathbf{n}_0, t) = 8t^2 r_2 \left( \frac{1 + \sqrt{\frac{\mathbf{n}_0}{4\pi}} [1 - \bar{\mathbf{n}}(\mathbf{n}_0, t)]}{2t}, 0 \right), \quad 1 \leq \bar{\mathbf{n}}(\mathbf{n}_0, t) \leq 1 + \sqrt{\frac{4\pi}{\mathbf{n}_0}}; \quad (2)$$

where

$$r_2(u, \theta) = \frac{\pi^2}{24} + \frac{u^2}{2} - \frac{\theta^2}{2} + \sum_{k=1}^{\infty} (-1)^k \frac{(e^{-2ku}) \cos(2k\theta)}{2k^2}; \quad u > 0; \quad -\frac{\pi}{2} \leq \theta < \frac{\pi}{2}. \quad (3)$$

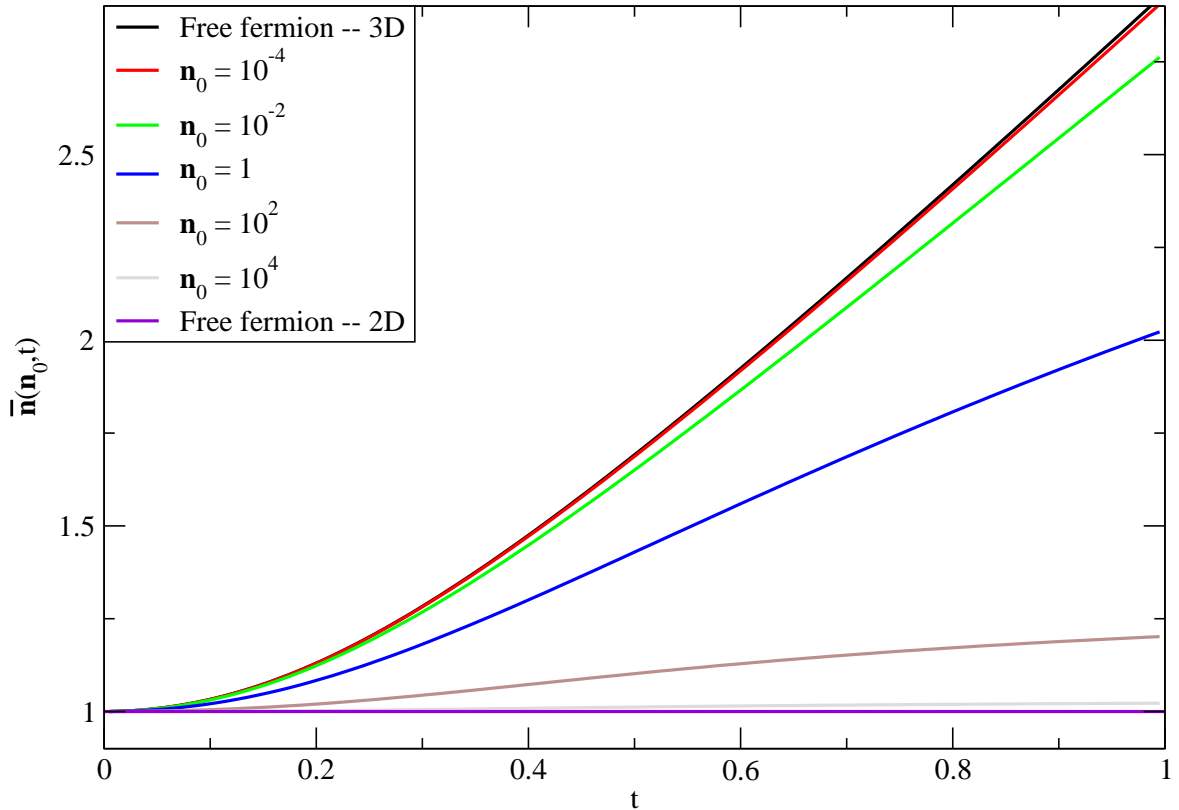


FIG. 1: Number density as a function of temperature for different choices of density at zero temperature.

This result for the number density is plotted as a function of temperature in Figure 1 and shows that it smoothly crosses over from a three dimensional free fermion gas as  $\mathbf{n}_0 \rightarrow 0$  to a two dimensional free fermion gas as  $\mathbf{n}_0 \rightarrow \infty$ .

The rest of the paper is organized as follows. We set up our notation for the three dimensional Thirring model and arrive at the saddle point equations in the limit of  $N \rightarrow \infty$  in Section II. The saddle point that dominates at all chemical potential and temperature is analyzed in Section III to obtain the main results stated above. Due to the involved interdependencies of the different saddle points at a fixed temperature and chemical potential, we revert to a graphical analysis in Section IV to show that the saddle point discussed in

Section III dominates at all chemical potential <sup>1</sup>.

## II. THE THREE DIMENSIONAL CONTINUUM THIRRING MODEL

The action for the continuum Thirring model in three Euclidean dimensions is given by

$$S(\bar{\psi}_i, \psi_i; \lambda) = \int d^3x \sum_{i=1}^N \bar{\psi}_i D(\mu) \psi_i + \frac{1}{2N\lambda} \int d^3x \sum_{k=1}^3 \left( \sum_{i=1}^N \bar{\psi}_i \sigma_k \psi_i \right)^2, \quad (4)$$

where

$$D(\mu) = \sum_{k=1}^3 \sigma_k \partial_k + \sigma_3 \mu \quad (5)$$

is the Dirac operator acting on a two-component fermion in a  $\ell^2 \times \beta$  periodic box and  $\mu$  is the chemical potential. The fermions obey periodic boundary conditions in the spatial directions and anti-periodic boundary conditions in the thermal direction. Upon introduction of a vector auxiliary field,  $V_k(x)$ , to replace the four-fermi interaction and a subsequent integration of the fermions results in

$$S(V_k, \lambda) = N \left[ \frac{\lambda}{2} \left( \int d^3x \sum_k V_k^2 \right) - \ln \det(D(V_k)) \right]; \quad (6)$$

where

$$D(V_k) = \sum_{k=1}^3 \sigma_k (\partial_k + iV_k) + \sigma_3 \mu \quad (7)$$

With  $V_k \rightarrow -V_k$  and  $x_k \rightarrow -x_k$ , we see that  $\mu \rightarrow -\mu$ . Therefore, it is sufficient to consider a positive value for the chemical potential in our analysis.

Assuming translational invariance to hold in the large  $N$  limit, we will analyze the action per flavor with the auxiliary field restricted to constants,

$$V_1(x) = \frac{2\pi h_1}{\ell}; \quad V_2(x) = \frac{2\pi h_2}{\ell}; \quad V_3(x) = \frac{2\pi h_3}{\beta}. \quad (8)$$

The minimum will occur at  $h_1 = h_2 = 0$  in the  $\ell \rightarrow \infty$  limit. One can use standard formulas in [28] to perform the sum over momentum in the  $\beta$  direction and the resulting action density (per unit spatial volume) per flavor is

$$S(h_3; T, \mu) = 2\pi^2 T h_3^2 - \frac{2T^2}{\pi} \int_0^\infty dx \, x \ln \frac{4 \cosh \left( x + i\pi h_3 + \frac{\mu}{2T} \right) \cosh \left( x - i\pi h_3 - \frac{\mu}{2T} \right)}{e^{2x}} \quad (9)$$

---

<sup>1</sup> *Much ado about nothing* – William Shakespeare.

The integration variable is related to the spatial momentum by  $x = \frac{\beta p}{2} = \frac{p}{2T}$  and we have set  $T$  and  $\mu$  in units of  $\lambda$ .

The action density is complex and we will perform a saddle point analysis. We elevate  $(2\pi h_3)$  to a complex variable  $z = \gamma + i\frac{\delta}{T}$  and define

$$\omega = u + i\theta; \quad u = \frac{\mu - \delta}{2T}; \quad \theta \in \left[ \frac{-\pi}{2}, \frac{\pi}{2} \right]; \quad z = -2i \left( \omega - \frac{\mu}{2T} + in\pi \right); \quad n \in \mathbf{I}. \quad (10)$$

The action density can be written in terms of polylogarithms [29] as

$$S(n, \omega; T, \mu) = S^b(n, \omega; T, \mu) + S^f(\omega; T, \mu); \quad (11)$$

$$S^b(n, \omega; T, \mu) = -2T \left( \omega - \frac{\mu}{2T} + in\pi \right)^2; \quad S^f(\omega; T, \mu) = \frac{T^2}{2\pi} \left[ \text{Li}_3(-e^{2\omega}) + \text{Li}_3(-e^{-2\omega}) \right]. \quad (12)$$

The partition function is given by

$$Z(T, \mu) = \sum_{n=-\infty}^{\infty} \int_{-\frac{i\pi}{2}}^{\frac{i\pi}{2}} d\omega e^{-N\ell^2 S(n, \omega; T, \mu)}. \quad (13)$$

The saddle points are given by  $\frac{dS(n, \omega; T, \mu)}{d\omega} = 0$  which we will label by  $\omega_n$  or  $(\theta_n, \delta_n)$  with the possibility that more than one saddle point exist at a fixed  $n$ .

The number density per flavor is given by

$$\begin{aligned} \mathbf{n}(T, \mu) &= \frac{T}{\ell^2 N} \frac{d \ln Z(T, \mu)}{d\mu} = -\frac{1}{2Z(T, \mu)} \sum_{n=-\infty}^{\infty} \int_{-\frac{i\pi}{2}}^{\frac{i\pi}{2}} d\omega \frac{dS_f(n, \omega; T, \mu)}{d\omega} e^{-N\ell^2 S(n, \omega; T, \mu)} \\ &= -\frac{1}{2Z(T, \mu)} \sum_{n=-\infty}^{\infty} \int_{-\frac{i\pi}{2}}^{\frac{i\pi}{2}} d\omega \left( 4T \left( \omega - \frac{\mu}{2T} + in\pi \right) + \frac{dS(n, \omega; T, \mu)}{d\omega} \right) e^{-N\ell^2 S(z; T, \mu)}. \end{aligned} \quad (14)$$

### A. Equations for saddle points

The complex valued equation for the saddle point using polylogarithm identities is

$$\begin{aligned} \frac{\mu}{2T} &= \omega_n + in\pi + \frac{T}{4\pi} \left[ \text{Li}_2(-e^{-2\omega_n}) - \text{Li}_2(-e^{2\omega_n}) \right] \\ &= \begin{cases} \frac{\pi T}{24} + \omega_n + in\pi + \frac{T}{2\pi} \omega_n^2 + \frac{T}{2\pi} \sum_{k=1}^{\infty} (-1)^k \frac{e^{-2k\omega_n}}{k^2}; & u_n > 0 \\ -\frac{\pi T}{24} + \omega_n + in\pi - \frac{T}{2\pi} \omega_n^2 - \frac{T}{2\pi} \sum_{k=1}^{\infty} (-1)^k \frac{e^{2k\omega_n}}{k^2}; & u_n < 0 \end{cases}. \end{aligned} \quad (15)$$

For the purpose of analysis, we separate the above equation into its real and imaginary part as

$$\begin{aligned}\frac{\pi(\theta_n + n\pi)}{T} &= r_1(|u_n|, \theta_n) = -|u_n|\theta_n + \sum_{k=1}^{\infty} (-1)^k \frac{e^{-2k|u_n|} \sin(2k\theta_n)}{2k^2}; \\ \frac{\pi\mu}{2T^2} &= \frac{u_n}{|u_n|} \left[ \frac{\pi|u_n|}{T} + r_2(|u_n|, \theta_n) \right] \\ r_2(|u_n|, \theta_n) &= \frac{\pi^2}{24} + \frac{u_n^2}{2} - \frac{\theta_n^2}{2} + \sum_{k=1}^{\infty} (-1)^k \frac{(e^{-2k|u_n|}) \cos(2k\theta_n)}{2k^2}.\end{aligned}\quad (16)$$

The real and imaginary parts of the action density needed to study the dominance of one saddle point over another are

$$\begin{aligned}S_R^b(n, \theta, \delta; T, \mu) &= 2T(\theta + n\pi)^2 - \frac{\delta^2}{2T} \\ S_R^f(\theta, \delta; T, \mu) &= \frac{2T^2}{\pi} \left[ |u| \left( \theta^2 - \frac{\pi^2}{12} \right) - \frac{|u|^3}{3} + \sum_{k=1}^{\infty} (-1)^k \frac{e^{-2k|u|} \cos(2k\theta)}{2k^3} \right] \\ S_I^b(n, \theta, \delta; T, \mu) &= 2\delta(\theta + n\pi) \\ S_I^f(\theta, \delta; T, \mu) &= -\frac{u}{|u|} \frac{2T^2}{\pi} \left[ \frac{\theta^3}{3} - \frac{\pi^2\theta}{12} + u^2\theta + \sum_{k=1}^{\infty} (-1)^k \frac{e^{-2k|u|} \sin(2k\theta)}{2k^3} \right].\end{aligned}\quad (17)$$

Referring to Eq. (A3), we note that the derivative of  $r_1(|u|, \theta)$  with respect to  $\theta$  at  $\theta = 0$  is negative. The derivative can become zero at most once for  $|\theta| < \frac{\pi}{2}$ , if  $|u| < u_0 = \frac{1}{2} \ln \frac{3+\sqrt{5}}{2}$ . Referring to Eq. (A1), we conclude that  $r_1(|u|, \theta)$  is positive for  $-\frac{\pi}{2} \leq \theta < 0$  and negative for  $0 < \theta \leq \frac{\pi}{2}$ . There is always a saddle point with  $n = 0$  and it has  $\theta_0 = 0$ . For  $n \neq 0$ , the saddle point, if one exists, will be in the region  $-\frac{\pi}{2} \leq \theta_n < 0$  if  $n > 0$  and will be in the region  $0 < \theta_n \leq \frac{\pi}{2}$  if  $n < 0$ .

Assuming the saddle point at  $n = 0$  dominates, the result for the number density will be

$$\mathbf{n}(T, \mu) = \delta_0. \quad (18)$$

Let us assume we have a solution to the saddle point equations given by  $(\theta_n, \delta_n)$  with  $n > 0$ . Since

$$r_1(|u_n|, -\theta_n) = -r_1(|u_n|, \theta_n); \quad r_2(|u_n|, -\theta_n) = r_2(|u_n|, \theta_n), \quad u_{-n} = u_n \quad (19)$$

we can conclude that  $(\theta_{-n}, \delta_{-n}) = (-\theta_n, \delta_n)$  is a saddle point with  $-n < 0$ . It follows from Eq. (17) that

$$S_R(n, \theta_n, \delta_n; T, \mu) = S_R(-n, \theta_{-n}, \delta_{-n}; T, \mu); \quad S_I(n, \theta_n, \delta_n; T, \mu) = -S_I(-n, \theta_{-n}, \delta_{-n}; T, \mu). \quad (20)$$

If this pair of saddle points were to dominate over the solitary one at  $n = 0$ , the number density will be

$$\mathbf{n}(T, \mu) = \delta_n - 2(\theta_n + n\pi)T \tan[N\ell^2 S_I(n, \theta_n, \delta_n; T, \mu)] \quad (21)$$

which does not have a smooth  $N \rightarrow \infty$  limit.

### III. ANALYSIS ASSUMING THE SADDLE POINT AT $n = 0$ DOMINATES

The only equation is

$$\frac{\pi\mu}{2T^2} = \frac{u_0}{|u_0|} \left[ \frac{\pi|u_0|}{T} + r_2(|u_0|, 0) \right]. \quad (22)$$

Referring to Eq. (A2), we have  $r_2(|u_0|, 0) > 0$  which results in

$$u_0 > 0; \quad \delta_0 = \frac{2T^2}{\pi} r_2\left(\frac{\mu - \delta_0}{2T}, 0\right). \quad (23)$$

Rewriting the saddle point equation as

$$\frac{\mu}{T^2} - \frac{2u_0}{T} = \frac{2}{\pi} r_2(u_0, 0); \quad u_0 = \frac{\mu - \delta_0}{2T} > 0. \quad (24)$$

we see there is one and only one solution for  $u_0$  such that  $0 \leq u_0 \leq \frac{\mu}{2T}$  ( $0 \leq \delta_0 \leq \mu$ ). Using Eq. (A3), we obtain

$$\frac{\partial \delta_0}{\partial T} = \frac{2T 2r_2(u_0, 0) + u_0 d_1(u_0, 0)}{\pi \left(1 - \frac{T}{\pi} d_1(u_0, 0)\right)}. \quad (25)$$

We note from Eq. (A2) and Eq. (A3) that

$$d_1(u_0, 0) < 0; \quad 2r_2(u_0, 0) + u_0 d_1(u_0, 0) = u_0 \ln(1 + e^{-2u_0}) + 4 \int_0^{u_0} dx \frac{x}{1 + e^{2x}} > 0. \quad (26)$$

Therefore we conclude that  $\frac{\partial \delta_0}{\partial T} > 0$  and  $\delta_0$  is a monotonically increasing function of temperature at a fixed chemical potential.

Assuming that the saddle point at  $n = 0$  dominates at all chemical potential and temperature, the number density is given by  $\mathbf{n} = \delta_0$ . Since

$$\lim_{T \rightarrow 0} \frac{2T^2}{\pi} r_2(u_0, 0) = \frac{(\mu - \delta_0)^2}{4\pi}. \quad (27)$$

the saddle point equation as  $T \rightarrow 0$  is

$$\mathbf{n}_0 = \frac{(\mu - \mathbf{n}_0)^2}{4\pi}, \quad (28)$$

which results in the number density at  $T = 0$  to be

$$\mathbf{n}_0 = \mu + 2\pi \left( 1 - \sqrt{1 + \frac{\mu}{\pi}} \right). \quad (29)$$

We can trade the chemical potential for  $\mathbf{n}_0$  using

$$\mu = \mathbf{n}_0 + \sqrt{4\pi\mathbf{n}_0}. \quad (30)$$

To see the relevance of the Thirring coupling, we define a reduced temperature by  $T = \sqrt{4\pi\mathbf{n}_0}t$  and write the number density at any temperature as  $[\bar{\mathbf{n}}(\mathbf{n}_0, t)\mathbf{n}_0]$ , noting that  $\bar{\mathbf{n}}$  will depend on  $\mathbf{n}_0$  in addition to  $t$ . It is this dependence that shows the relevance of the Thirring coupling. Referring to Eq. (23) and Eq. (30) we arrive at

$$\bar{\mathbf{n}}(\mathbf{n}_0, t) = 8t^2 r_2 \left( \frac{1 + \sqrt{\frac{\mathbf{n}_0}{4\pi}} [1 - \bar{\mathbf{n}}(\mathbf{n}_0, t)]}{2t}, 0 \right). \quad (31)$$

One can either use Eq. (16) or Eq. (A2) and see that the above equation reduces to a free fermion behavior in three dimensions as  $\mathbf{n}_0 \rightarrow 0$ . Using Eq. (A2) and Eq. (24), the asymptotic behavior in  $t$  at a fixed  $\mathbf{n}_0$  is

$$\bar{\mathbf{n}}(\mathbf{n}_0, t) = 1 + \sqrt{\frac{4\pi}{\mathbf{n}_0}} - \frac{\pi \left( 1 + \sqrt{\frac{4\pi}{\mathbf{n}_0}} \right)}{(\ln 2)\sqrt{4\pi\mathbf{n}_0}} \frac{1}{t} + O(t^{-2}). \quad (32)$$

Since the number density monotonically increases with temperature at a fixed  $\mathbf{n}_0$ , it is bounded by

$$1 \leq \bar{\mathbf{n}}(\mathbf{n}_0, t) \leq 1 + \sqrt{\frac{4\pi}{|\mathbf{n}_0|}} \quad (33)$$

The density does not change with temperature in the limit  $\mathbf{n}_0 \rightarrow \infty$  and this is the free fermion behavior in two dimensions. The sub-leading term for small  $t$  is

$$\bar{\mathbf{n}}(\mathbf{n}_0, t) = 1 + \frac{\pi^2}{3} \frac{1}{1 + \sqrt{\frac{\mathbf{n}_0}{\pi}}} t^2 + O(t^3). \quad (34)$$

A plot of  $\bar{\mathbf{n}}(\mathbf{n}_0, t)$  as a function of  $t$  has already been shown in Figure 1 at several different values of  $\mathbf{n}_0$  to demonstrate the crossover from three dimensional free fermion behavior as  $\mathbf{n}_0 \rightarrow 0$  to two dimensional free fermion behavior as  $\mathbf{n}_0 \rightarrow \infty$ .

#### IV. NON-DOMINANCE OF THE SADDLE POINTS AT $n \neq 0$

We will only consider  $n > 0$  since we have shown at the end of Section II A that saddle points at  $n$  and  $(-n)$  are paired. Then every solution has to satisfy  $-\frac{\pi}{2} \leq \theta_n \leq 0$ . We will



fix the temperature and use  $\theta_n$  instead of chemical potential since it is more convenient from the viewpoint of solving the saddle point equations. We will graphically demonstrate the non-dominance of the saddle points at  $n \neq 0$  by defining

$$\Delta(n, \theta_n, T) = \frac{S_R(n, \theta_n, \delta_n(\theta_n); \mu(\theta_n), T) - S_R(0, 0, \delta_0(\theta_n); \mu(\theta_n), T)}{2Tn^2\pi^2} \quad (35)$$

and showing that it remains positive at all  $n, T$  and allowed values of  $\theta_n \in [-\frac{\pi}{2}, 0]$ . To this end we will use the following steps:

1. We will show that  $\mu \rightarrow \infty$  as  $\theta_n \rightarrow 0$  at all temperatures.
2. There exists a temperature  $T_0(n)$  above which a certain region given by  $-\frac{\pi}{2} < \theta_l(T) < \theta_n < \theta_r(T) < 0$  has no solution to the saddle point equations. The chemical potential will monotonically increase from 0 to  $\infty$  as  $\theta_n$  increases from  $\theta_r(T)$  to 0 and it will monotonically increase from 0 to a finite non-zero value as  $\theta_n$  decreases from  $\theta_l(T)$  to  $-\frac{\pi}{2}$ . Furthermore,  $\theta_l(T_0(n)) = \theta_r(T_0(n)) = \theta_0(n)$ .
3. There exists a temperature  $T_1(n)$  below which the chemical potential will monotonically decrease from  $\infty$  to a finite non-zero value as  $\theta_n$  decreases from 0 to  $-\frac{\pi}{2}$ . In other words there will be a region of chemical potential given by  $0 \leq \mu < \mu_1(T)$  for which there is no solution to the saddle point equations. Furthermore,  $\mu_1(T_1(n)) = 0$ .
4. We will explicitly study the case of zero temperature and the case of zero chemical potential.
5. Even though  $\Delta(n, \theta_n, T)$  will not be monotonic in  $\theta_n$  at a fixed  $n$  and temperature, it reaches an absolute minimum at  $\theta = -\frac{\pi}{2}$  at all  $n$  and temperatures. We will study  $\Delta(n, -\frac{\pi}{2}, T)$  as a function of  $T$  and show that the minimum at each  $n$  is larger than zero for all  $n$ .

**A.**  $\theta_n \rightarrow 0_- \Rightarrow \mu \rightarrow \infty$ :

Keeping terms to relevant orders in  $\theta_n$  and using Eq. (A3), the first equation in Eq. (16) results in

$$|u_n| = -\frac{n\pi^2}{T\theta_n} - \frac{\pi}{T} + O\left(e^{\frac{1}{\theta_n}}\right). \quad (36)$$

Inserting this into the second equation in Eq. (16) results in

$$u_n > 0; \quad \mu = \frac{n^2 \pi^3}{\theta_n^2} + \frac{\pi T^2}{12} - \pi + O(\theta_n^2). \quad (37)$$

If we use the diverging chemical potential with the leading correction into Eq. (24), we find that  $u_0 = u_n$  up to the two correction terms. Therefore, we arrive at

$$\Delta(n, 0_-, T) = 1, \quad (38)$$

and the saddle point at  $n = 0$  dominates as  $\mu \rightarrow \infty$  for all values of temperature.

### B. $T_0(n)$ :

Noting that  $d_2(|u|, \theta) > 0$  for  $-\frac{\pi}{2} < \theta < 0$ , the right hand side of the first equation in Eq. (16) monotonically increases with  $|u|$  at a fixed  $\theta$ . Therefore, at every value of  $\theta$ , the lowest value of the right hand side is given by  $r_1(0, \theta)$ . If the temperature is above a certain value, we will have a region of  $\theta$  where there is no solution to the first equation in Eq. (16). This transition temperature is the solution to

$$\frac{\pi}{T_0(n)} (\theta_0(n) + n\pi) = r_1(0, \theta_0(n)); \quad \frac{\pi}{T_0(n)} = -\ln[2 \cos \theta_0(n)], \quad (39)$$

which results in

$$\begin{aligned} \theta_0(1) &= -0.372690809 \pi; & \theta_0(2) &= -0.350144201 \pi; & \theta_0(5) &= -0.339555189 \pi \\ T_0(1) &= 12.563174152; & T_0(2) &= 2 \times 16.123729198; & T_0(5) &= 5 \times 18.139848147; \end{aligned} \quad (40)$$

and

$$\theta_0(\infty) = \frac{\pi}{3}; \quad \lim_{n \rightarrow \infty} \frac{T_0(n)}{n} = \frac{\pi^2}{r_1(0, \frac{\pi}{3})} = 19.448615248. \quad (41)$$

Since  $u_n = 0$  at this temperature,  $T_0(n)$ , and  $\theta_0(n)$  we have  $r_2(0, \theta_0(n)) = 0$  and  $\mu = 0$  at this point.

After fixing the temperature, we choose a  $\theta_n$  in the allowed region and solve for  $|u_n|$  using the first equation in Eq. (16) and then solve for the chemical potential using the second equation. Referring to Eq. (A3), we note that  $d_2(|u|, \theta)$  remains non-negative in  $-\frac{\pi}{2} \leq \theta_n \leq 0$  and we conclude that  $r_2(|u|, \theta)$  is a monotonically increasing function in  $-\frac{\pi}{2} \leq \theta_n \leq 0$ . Since we are only considering  $\mu > 0$ , we can conclude from the second equation

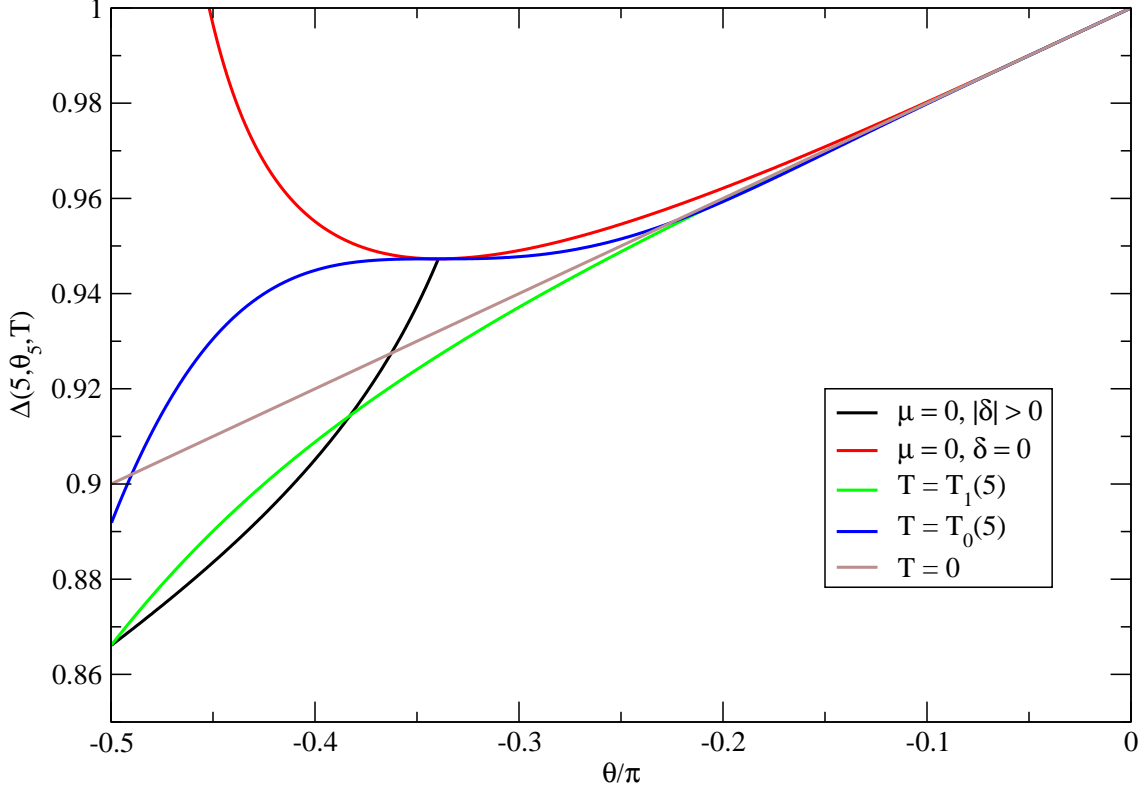


FIG. 2: The action at the  $n = 5$  saddle point is taken as a typical example since it has all the features for a generic  $n$  and it is compared with the  $n = 0$  saddle point to show that the  $n = 0$  saddle point dominates at all temperatures and chemical potential. This plot shows the comparison at some specific values of temperature and also at zero chemical potential.

in Eq. (16) that  $u_n > 0$  if  $\left[ \frac{\pi|u_n|}{T} + r_2(|u_n|, \theta_n) \right] > 0$  and  $u_n < 0$  if  $\left[ \frac{\pi|u_n|}{T} + r_2(|u_n|, \theta_n) \right] < 0$ . Furthermore, we can have a solution to the saddle point equations with  $n > 0$  and  $\mu = 0$  only if  $\left[ \frac{\pi|u_n|}{T} + r_2(|u_n|, \theta) \right] = 0$ . We have used  $n = 5$  as a typical value of  $n$  and plotted  $\Delta(5; \theta_5, T_0(5))$  as a blue curve in Figure 2. We see it remains positive in the entire range of  $\theta_5$  showing that the saddle at  $n = 0$  dominates over  $n = 5$  at  $T_0(5)$ .

**C.  $T_1(n)$ :**

Consider moving down from  $\theta_n = 0$ . Noting that  $u_n$  is positive to start with and noting that  $d_2(|u|, \theta)$  is positive in  $-\frac{\pi}{2} \leq \theta_n \leq 0$ , we conclude from Eq. (A5) that  $\mu$  decreases as  $\theta_n$  moves down from zero as long as  $u_n$  remains positive. At  $\theta_n = -\frac{\pi}{2}$ , the first equation in Eq. (16) reduces to

$$|u_n| = \frac{(2n-1)\pi}{T} \quad (42)$$

and the condition for  $\left[\frac{\pi|u_n|}{T} + r_2(|u_n|, -\frac{\pi}{2})\right]$  to remain positive is

$$\frac{\pi^2}{T^2}(4n^2 - 1) - \frac{\pi^2}{6} + \sum_{k=1}^{\infty} \frac{e^{-\frac{2(2n-1)k\pi}{T}}}{k^2} > 0. \quad (43)$$

This gives the condition for  $\mu = 0$  to occur for  $T > T_n(n)$  with

$$\begin{aligned} T_1(1) &= 4.654727000; & T_1(2) &= 2 \times 4.987847524; \\ T_1(5) &= 5 \times 5.044788571; & \lim_{n \rightarrow \infty} \frac{T_1(n)}{n} &= 5.028967463. \end{aligned} \quad (44)$$

We have plotted  $\Delta(5; \theta_5, T_1(5))$  as a red curve in Figure 2. We see it remains positive in the entire range of  $\theta_5$  showing that the saddle at  $n = 0$  dominates over  $n = 5$  at  $T_1(5)$ .

**D.  $T = 0$ :**

Let us consider the limit  $T \rightarrow 0$ . The two saddle point equations in Eq. (16) sequentially result in

$$\lim_{T \rightarrow 0} T|u_n| = -\frac{\pi(\theta_n + n\pi)}{\theta_n}; \quad \lim_{T \rightarrow 0} T^2 \left[ \frac{\pi|u_n|}{T} + r_2(|u_n|, \theta_n) \right] = \frac{\pi^2(n^2\pi^2 - \theta_n^2)}{2\theta_n^2} > 0; \quad (45)$$

and we obtain

$$\mu = \frac{\pi(n^2\pi^2 - \theta_n^2)}{\theta_n^2}; \quad \delta_n = \frac{\pi(\theta_n + n\pi)^2}{\theta_n^2}. \quad (46)$$

With this choice of  $\mu$ , the saddle point solution with  $n = 0$  is given by

$$\lim_{T \rightarrow 0} T u_0 = -\frac{\pi(\theta_n + n\pi)}{\theta_n}; \quad \delta_0 = \frac{\pi(\theta_n + n\pi)^2}{\theta_n^2}, \quad (47)$$

and we conclude

$$\Delta(n, \theta_n, 0) = 1 + \frac{\theta_n}{n\pi}. \quad (48)$$

We have plotted  $\Delta(5, \theta_5, 0)$  for reference in Figure 2 as a brown line.

**E.  $\mu = 0$ :**

If  $T > T_1(n)$  we have a saddle point solution with  $\mu = 0$  and  $n > 0$ . Setting  $\mu = 0$ , we first note by referring to Eq. (23) that the saddle point with  $n = 0$  corresponds to  $u_0 = 0$  and therefore  $\delta_0 = 0$  and the real part of the action at the  $n = 0$  saddle point is (referring to Eq. (17))

$$S_R(0, 0, 0; 0, T) = \frac{2T^2}{\pi} \sum_{k=1}^{\infty} \frac{(-1)^k}{2k^3} = -\frac{3\zeta(3)}{4\pi} T^2. \quad (49)$$

Referring to Eq. (16), the solution to the saddle points at  $n > 0$  is given by

$$f(|u_n|, \theta_n) = |u_n| r_1(|u_n|, \theta_n) + (\theta_n + n\pi) r_2(|u_n|, \theta_n) = 0. \quad (50)$$

Viewing the above equation as a function of  $|u_n|$  at a fixed  $\theta_n$  we note that  $|u_n| = 0$  is a solution to the above equation. In this case,  $\delta_n = 0$  and the temperature as a function of  $\theta_n$  from the first equation in Eq. (16) is

$$T_n(\theta_n) = \frac{\pi(\theta_n + n\pi)}{r_1(0, \theta_n)}, \quad (51)$$

and

$$\Delta(n, \theta_n, T_n(\theta_n)) = \left[\frac{\theta_n}{n\pi} + 1\right]^2 + \frac{T_n(\theta_n)}{2n^2\pi^3} J_f(\theta_n); \quad J_f(\theta) = \sum_{k=1}^{\infty} (-1)^k \frac{\cos(2k\theta) - 1}{k^3}. \quad (52)$$

Noting that

$$J_f\left(-\frac{\pi}{2}\right) = \frac{7\zeta(3)}{4} > 0; \quad J_f(0) = 0. \quad (53)$$

and noting that

$$\frac{dJ_f(\theta)}{d\theta} = 2\text{Cl}_2(\pi - 2\theta) \leq 0, \quad (54)$$

where  $\text{Cl}_2$  is the Clausen function of order 2, we conclude that  $J_f(\theta)$  is non-negative in  $-\frac{\pi}{2} < \theta_n < 0$ . Therefore, these saddle points at  $n > 0$  and  $\mu = 0$  do not dominate over  $n = 0$ . We have plotted  $\Delta(5, \theta_5, T)$  for  $\mu = 0$  and  $\delta_5 = 0$  as a red curve in Figure 2. Note that the divergence in  $\Delta(5, \theta_5, T)$  as  $\theta_5 \rightarrow -\frac{\pi}{2}$  can be seen from Eq. (52) and Eq. (53).

There is another solution to Eq. (50) with  $|u_n| > 0$  if  $T_1(n) < T < T_0(n)$  and  $\theta_n < \theta_0(n)$ . To see this note that the derivative of Eq. (50) with respect to  $|u_n|$  gives us

$$\frac{\partial f(|u_n|, \theta_n)}{\partial |u_n|} = r_1(|u_n|, \theta_n) + |u_n| d_2(|u_n|, \theta_n) - (\theta_n + n\pi) d_1(|u_n|, \theta_n). \quad (55)$$

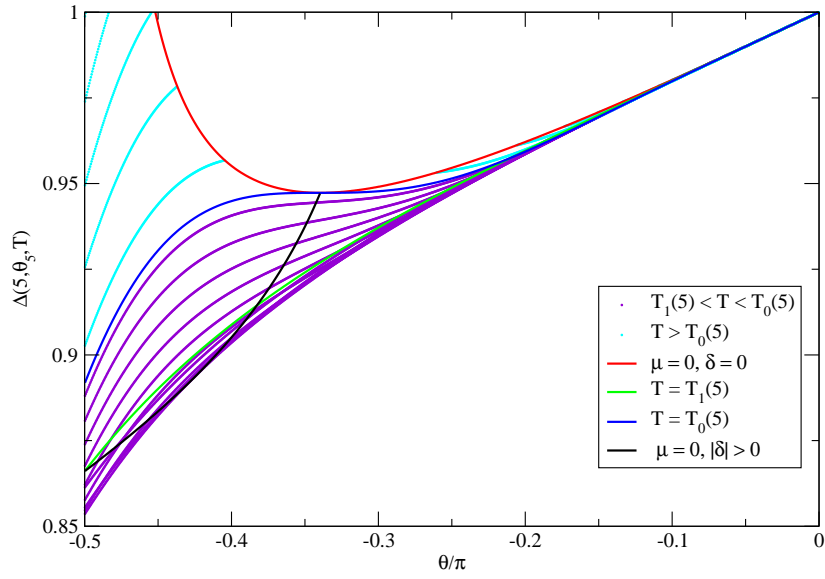
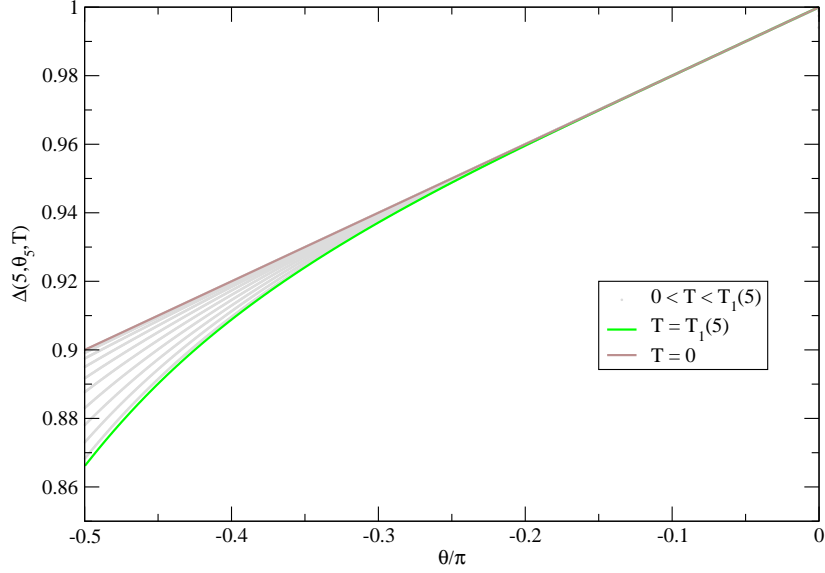


FIG. 3: The top plot shows that the difference between  $T = 0$  and  $T = T_1(5)$  is bounded by the two extremes. The bottom plot shows that the difference between  $T = T_1(5)$  and  $T = T_0(5)$  moves smoothly from one end to the other but there is a temperature in between the two ends where the difference is smallest as a function of  $\theta_n$ . On the other hand, the difference for  $T > T_0(5)$  is bounded from below by  $T = T_0(5)$ .

The first two terms are positive in the range  $-\frac{\pi}{2} < \theta_n < 0$ . Furthermore,  $d_1(|u_n|, \theta_n)$  is positive only if  $-\frac{\pi}{2} < \theta_n < -\frac{\pi}{6}$ . We can see that  $f(0, \theta_n) = 0$  and  $f(|u_n|, \theta_n)$  goes as  $[\frac{n\pi - \theta_n}{2} u_n^2]$  as  $|u_n| \rightarrow \infty$ . If  $\frac{\partial f(0, \theta_n)}{\partial |u_n|} > 0$  the only solution to Eq. (50) is  $|u_n| = 0$ . The condition for  $\frac{\partial f(0, \theta_n)}{\partial |u_n|} = 0$  is the same as Eq. (39) and therefore we conclude that  $-\frac{\pi}{2} < \theta_n < \theta_0(n)$  for a solution to Eq. (50) to exist with  $|u_n| \neq 0$ . We have plotted  $\Delta(5, \theta_5, T)$  for  $\mu = 0$  and  $\delta_5 \neq 0$  as a black curve in Figure 2 and it meets the red curve at  $\theta_0(5)$ . Note that the temperature along the black curve changes from  $T = T_1(5)$  at  $\theta_5 = -\frac{\pi}{2}$  to  $T = T_0(5)$  at  $\theta_5 = \theta_0(5)$ . A generic feature of the curves shown in Figure 2 is the intersection of the black curve ( $\mu = 0$  and  $\delta_5 \neq 0$ ) with the green curve ( $T_1(5)$ ) at a value of  $\theta_n$  away from  $-\frac{\pi}{2}$ . The temperature and chemical potential on the two curves at the intersection point are different but yield the same value for  $\Delta(n, \theta_n, T)$ .

#### F. Analysis at $\theta_n = -\frac{\pi}{2}$ :

The two plots in Figure 3 shows the behavior of  $\Delta(5, \theta_5, T)$  as a function of  $\theta_5$  over the entire range of  $T$ . For  $T < T_1(n)$ , we find a solution in the entire range of  $\theta_n$  with  $\mu$  monotonically increasing from a positive finite value at  $\theta_n = -\frac{\pi}{2}$  to a divergence at  $\theta_n = 0$ . The grey points in the top plot of Figure 3 shows  $\Delta(1, \theta_1, T)$  for  $T < T_1(n)$  and all points lie between the line at  $T = 0$  and  $T = T_1(1)$  and moves continuously from one to the other as  $T$  changes. For  $T_1(n) < T < T_0(n)$ , we again find a solution in the entire range of  $\theta_n$ . But we find a  $\theta_0(T)$  at which  $\mu = 0$ . The chemical potential monotonically decreases from a positive finite value at  $\theta_n = -\frac{\pi}{2}$  to zero at  $\theta_n = \theta_0(T)$  and then monotonically increases to a divergence at  $\theta_n = 0$ . Furthermore,  $\theta_0(T_1(n)) = -\frac{\pi}{2}$  and  $\theta_0(T_0(n)) = \theta_0(n)$ . These features are shown in the bottom plot of Figure 3. The curves for  $\Delta(5, \theta_5, T)$  at a fixed  $T$  in  $T_1(5) < T < T_0(5)$  are shown by violet points. Note that there is a range of  $T$  starting from  $T_1(5)$  where the curve intersects the black curve ( $\mu = 0$  and  $\delta_5 \neq 0$ ) at two points. Only one of the intersection points has the same temperature and chemical potential. Initially, it is the intersection point closer to  $\theta_5 = -\frac{\pi}{2}$  till the violet curve is tangential to the black curve. After that, the intersection point closer to  $\theta_0(5)$  is where the temperature and chemical potential matches. For  $T > T_0(5)$ , there will be a solution only if  $\theta_5$  does not belong to the interval  $(\theta_l(T), \theta_r(T))$  which can be obtained by setting the left hand side to  $T$  in Eq. (51). The chemical potential will monotonically decrease from a positive finite value at  $\theta_n = -\frac{\pi}{2}$  to

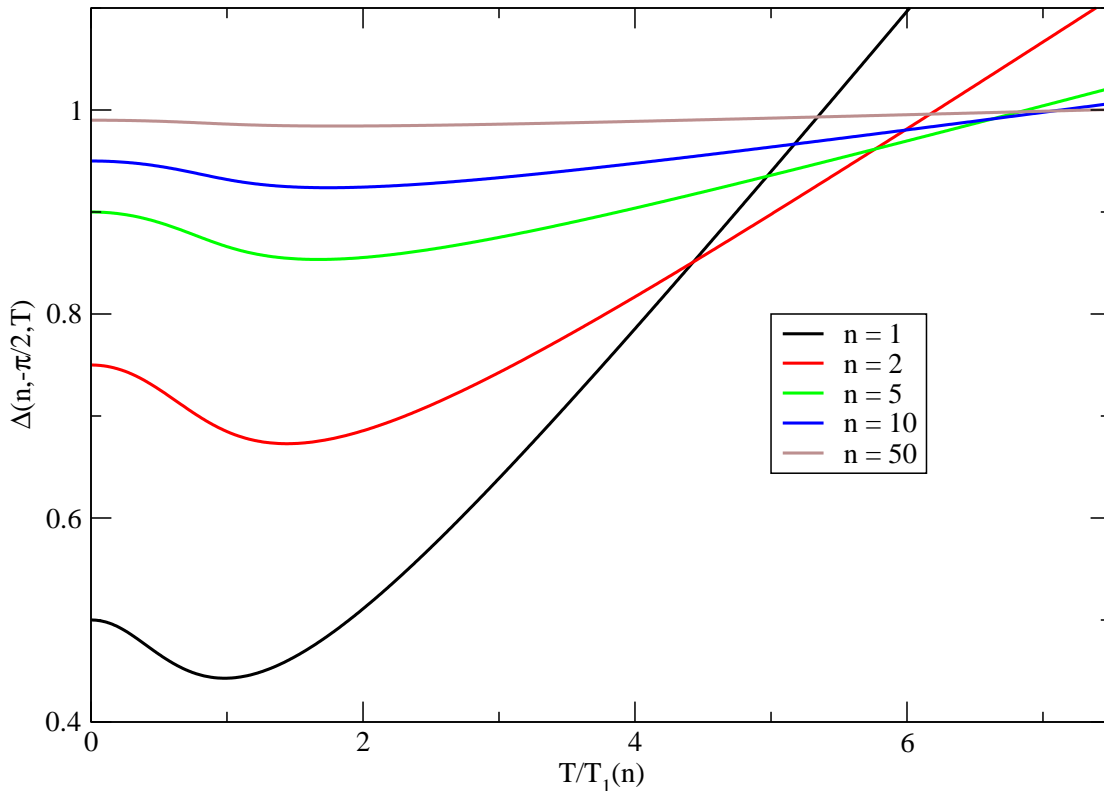


FIG. 4: The difference in the action between  $n > 0$  and  $n = 0$  at  $\theta_n = -\frac{\pi}{2}$  is plotted as a function of  $T/T_1(n)$ .

zero at  $\theta_l(T)$  and then monotonically increase from zero at  $\theta_r(T)$  to a divergence at  $\theta_n = 0$ . These features are also shown in the bottom plot of Figure 3 and we see that  $\Delta(5, \theta_5, T)$  for  $T > T_0(5)$  shown by cyan points lies above the curve at  $T = T_0(5)$  and has two parts. The boundary of the two parts is the red curve with  $\mu = 0$  and  $\delta = 0$ .

The graphical analysis discussed before specifically for  $n = 5$  enables us to conclude that  $\Delta(5, \theta_5, T)$  reaches a minimum at  $\theta_5 = -\frac{\pi}{2}$  at any fixed temperature. We therefore plot  $\Delta(n, -\frac{\pi}{2}, T)$  as a function of  $T$  for  $n = 1, 2, 5, 10, 50$  in Figure 4. The minimum occurs very close to  $T = T_1(1)$  but moves to a higher temperature with respect to  $T_1(n)$  as  $n$  is increased. The global minimum occurs at a finite value of  $T/T_1(n)$  even as  $n \rightarrow \infty$ . This plot along with the analysis done specifically for  $n = 5$  in Figure 2 and Figure 3 serves to graphically



prove our main point – the saddle point at  $n = 0$  dominates at all chemical potential and temperature.

## V. CONCLUSIONS

We have studied the three dimensional (two spatial and one thermal) Euclidean Thirring model at finite temperature and chemical model in the limit of infinite number of flavors and our aim was to understand the relevance of the Thirring coupling. The effective action is complex and we had to perform an extensive graphical analysis to show that one particular saddle point dominates over all other possible saddle points at all chemical potential and temperature. The relevance of the Thirring coupling is seen in the dependence of the behavior of the number density as a function of temperature on different values of the number density at zero temperature. The number density as a function of temperature behaves like a three dimensional free fermion gas as the number density at zero temperature approaches zero and it behaves like a two dimensional free fermion gas as the number density at zero temperature approaches infinity. The number density at a fixed non-zero value at zero temperature is a monotonically increasing function of temperature reaching a finite value at infinite temperature. The function for any given non-zero value of density at zero temperature smoothly interpolates between the two extremal behavior at zero number density and infinite number density at zero temperature.

### Acknowledgments

The author acknowledges partial support by the NSF under grant number PHY-1913010.

### Appendix A: Some useful properties of $r_1(u, \theta)$ and $r_2(u, \theta)$

We note that

$$r_1(|u|, 0) = 0; \quad r_1\left(|u|, \pm\frac{\pi}{2}\right) = \mp\frac{\pi|u|}{2}. \quad (\text{A1})$$

Using Riemann and Dirchlet zeta function formulas [29], we also note that

$$r_2(|u|, 0) = \frac{u^2}{2} + \int_0^{|u|} dx \ln(1 + e^{-2x}); \quad r_2\left(|u|, \pm\frac{\pi}{2}\right) = \frac{u^2}{2} + \int_0^{|u|} dx \ln(1 - e^{-2x}). \quad (\text{A2})$$

The derivatives of  $r_1(|u|, \theta)$  and  $r_2(|u|, \theta)$  with respect to  $|u|$  and  $\theta$  are

$$\begin{aligned}\frac{\partial r_1(|u|, \theta)}{\partial \theta} &= -\frac{\partial r_2(|u|, \theta)}{\partial |u|} = -\frac{1}{2} \ln [2 (\cosh(2u) + \cos(2\theta))] = d_1(u, \theta). \\ \frac{\partial r_1(|u|, \theta)}{\partial |u|} &= \frac{\partial r_2(|u|, \theta)}{\partial \theta} = -\tan^{-1} (\tanh |u| \tan \theta) = d_2(|u|, \theta).\end{aligned}\tag{A3}$$

Referring to the solutions as  $\theta_n(\mu)$ ,  $\delta_n(\mu)$  and  $u_n(\mu)$  we compute expressions for the derivative of  $\delta_n$  with respect to  $\mu$ . Noting that

$$\frac{\partial |u_n|}{\partial \mu} = \frac{u_n}{|u_n|} \frac{1}{2T} \left( 1 - \frac{\partial \delta_n}{\partial \mu} \right).\tag{A4}$$

and referring to Eq. (16), we obtain

$$\begin{aligned}\frac{\partial \theta_n}{\partial \mu} &= \frac{u_n}{|u_n|} \frac{\pi d_2}{2T^2 \left[ \left( \frac{\pi}{T} - d_1(|u_n|, \theta_n) \right)^2 + d_2^2(|u_n|, \theta_n) \right]}; \\ \frac{\partial \delta_n}{\partial \mu} &= 1 - \frac{\pi}{\pi - T d_1(|u_n|, \theta_n) + T \frac{d_2^2(|u_n|, \theta_n)}{\frac{\pi}{T} - d_1(|u_n|, \theta_n)}}.\end{aligned}\tag{A5}$$

- [1] G. Parisi, Nucl. Phys. **B100**, 368 (1975).
- [2] S. Hikami and T. Muta, Prog. Theor. Phys. **57**, 785 (1977).
- [3] Z. Yang (1990).
- [4] M. Gomes, R. Mendes, R. Ribeiro, and A. da Silva, Phys. Rev. D **43**, 3516 (1991).
- [5] S. Hands, Phys. Rev. D **51**, 5816 (1995), hep-th/9411016.
- [6] L. Del Debbio and S. Hands, Phys. Lett. B **373**, 171 (1996), hep-lat/9512013.
- [7] S. Hands (UKQCD), in *International Workshop on Perspectives of Strong Coupling Gauge Theories (SCGT 96)* (1996), pp. 383–389, hep-lat/9702003.
- [8] L. Del Debbio, S. Hands, and J. Mehegan (UKQCD), Nucl. Phys. B **502**, 269 (1997), hep-lat/9701016.
- [9] L. Del Debbio and S. Hands, Nucl. Phys. B **552**, 339 (1999), hep-lat/9902014.
- [10] S. Hands and B. Lucini, Phys. Lett. B **461**, 263 (1999), hep-lat/9906008.
- [11] S. Christofi, S. Hands, and C. Strouthos (2006), hep-lat/0703016.
- [12] S. Christofi, S. Hands, and C. Strouthos, Phys. Rev. D **75**, 101701 (2007), hep-lat/0701016.
- [13] H. Gies and L. Janssen, Phys. Rev. D **82**, 085018 (2010), 1006.3747.
- [14] L. Janssen and H. Gies, Phys. Rev. D **86**, 105007 (2012), 1208.3327.

- [15] D. Schmidt, B. Wellegehausen, and A. Wipf, PoS **LATTICE2015**, 050 (2016), 1511.00522.
- [16] B. H. Wellegehausen, D. Schmidt, and A. Wipf, Phys. Rev. D **96**, 094504 (2017), 1708.01160.
- [17] S. Hands, in *35th International Symposium on Lattice Field Theory* (2017), 1708.07686.
- [18] S. Hands, Phys. Rev. D **99**, 034504 (2019), 1811.04818.
- [19] S. Hands, PoS **Confinement2018**, 221 (2018).
- [20] J. J. Lenz, B. H. Wellegehausen, and A. Wipf, Phys. Rev. D **100**, 054501 (2019), 1905.00137.
- [21] N. Karthik and R. Narayanan, Phys. Rev. **D93**, 045020 (2016), 1512.02993.
- [22] N. Karthik and R. Narayanan, Phys. Rev. **D94**, 065026 (2016), 1606.04109.
- [23] N. Karthik and R. Narayanan, Phys. Rev. **D96**, 054509 (2017), 1705.11143.
- [24] N. Karthik and R. Narayanan, PoS **LATTICE2016**, 245 (2016), 1610.09355.
- [25] N. Karthik and R. Narayanan, Phys. Rev. Lett. **121**, 041602 (2018), 1803.03596.
- [26] N. Karthik and R. Narayanan (2019), 1908.05500.
- [27] M. Goykhman, JHEP **07**, 034 (2016), 1605.08449.
- [28] I. Gradshteyn and I. Ryzhik, Academic Press (2007).
- [29] DLMF, *NIST Digital Library of Mathematical Functions*, <http://dlmf.nist.gov/>, Release 1.0.26 of 2020-03-15, f. W. J. Olver, A. B. Olde Daalhuis, D. W. Lozier, B. I. Schneider, R. F. Boisvert, C. W. Clark, B. R. Miller, B. V. Saunders, H. S. Cohl, and M. A. McClain, eds., URL <http://dlmf.nist.gov/>.